Journal of Organometallic Chemistry, 427 (1992) 355–362
Elsevier Sequoia S.A., Lausanne
JOM 22426

Structure and Mössbauer effect study of $[Et_4N]_2[Fe_2(CO)_8]$

Juanita M. Cassidy, Kenton H. Whitmire
Department of Chemistry, Rice University, P.O. Box 1892, Houston, TX 77251 (USA)

and Gary J. Long
Department of Chemistry, University of Missouri — Rolla, Rolla, MO 65401 (USA)

(Received April 30, 1991; in revised form October 2, 1991)

Abstract

The reduction of $[Et_4N]_2[Pb\{Fe(CO)_4\}_3]$ leads to the well known $[Et_4N]_2[Fe_2(CO)_8]$ as determined by single crystal X-ray crystallography. The bis(tetraethylammonium)bis[tetracarbonylferrate(1−)], $C_{24}H_{40}Fe_2N_2O_8$, FW = 596.28 g/mol, monoclinic, $P2_1/n$ (#14), $a = 9.492(3)$, $b = 13.793(5)$, $c = 11.870(4)$ Å, $\beta = 112.81(2)°$, $V = 1432.5(8)$ Å^3, $D_x = 1.38$ g/cm^3, $Z = 2$, $\mu = 10.56$ cm^{-1}, λ(Mo-K_α) = 0.71069 Å, $F(000) = 628$, $T = 296$ K, $R = 0.032$, $R_w = 0.043$ for 1869 unique reflections with $I > 3\sigma(I)$. As in other salts, the anion of $[Et_4N]_2[Fe_2(CO)_8]$ consists of two iron atoms situated about a crystallographic inversion center, each of which is coordinated to four carbonyls in a trigonal bipyramidal fashion with the Fe–Fe bond in an axial site. Unexpectedly, the Fe–Fe distance, 2.841(1) Å, is significantly longer than reported for the $[PPN]^+ \cdot 2CH_3CN$, $[PPh_4]^+ \cdot 2CH_3CN$ and $[Fe(pyridine)_6]^{2+}$ salts. The Mössbauer effect spectra of the $[Et_4N]^+$ and $[PPN]^+$ salts, which have been measured at 78 and 296 K, are presented and discussed.

Introduction

Salts of the iron carbonyl anion $[Fe_2(CO)_8]^{2-}$ are commonly used reagents in the formation of organometallic derivatives [1]. The structure of $[Fe_2(CO)_8]^{2-}$ has been reported for acetonitrile solvated $[PPN]^+$ (bis(triphenylphosphine)iminium cation) [2] and $[PPh_4]^+$ salts [3]. The structure of the $[Fe(en)_3]^{2+}$ (en = ethylenediamine) salt has been determined but details have not been reported [4]. These Fe–Fe bond distances, which are the longest unsupported Fe–Fe bonds known (2.787(2), 2.792(1) and 2.75 Å, respectively), have been attributed to electrostatic repulsions between the two metal centers. Fe–Fe bond lengths, in general, cover a wide range of values from about 2.5 to 2.9 Å. In the course of our studies, we investigated the reduction of $[Et_4N]_2[Pb\{Fe(CO)_4\}_3]$ with sodium

Correspondence to: Dr. K.H. Whitmire, Department of Chemistry, Rice University, P.O. Box 1892, Houston, TX 77251, USA, or Dr. G.J. Long, Department of Chemistry, University of Missouri—Rolla, Rolla, MO 65401, USA.

naphthalenide and found the product to be $[Et_4N]_2[Fe_2(CO)_8]$. The structure has not been previously reported even though it is one of the most widely used salts. Surprisingly the Fe–Fe bond length in $[Et_4N]_2[Fe_2(CO)_8]$ is substantially longer than that found in the $[PPN]^+ \cdot 2CH_3CN$, $[Fe(en)_3]^{2+}$ and $[PPh_4]^+ \cdot 2CH_3CN$ derivatives. These differences may be chemically significant as studies have shown that the reactivity of charged organometallic compounds depends on the counter-ion involved as well as on ion-pairing effects [5,6]. Frequently reactions involving $[Fe_2(CO)_8]^{2-}$ are successful with one countercation, but not with another [1]. Our empirical observations are that $[Et_4N]^+$ salts are more reactive in general than the corresponding $[PPN]^+$ salts and the lengthening of the Fe–Fe bond, which we speculate to arise from differences in ion pairing capabilities of $[Et_4N]^+$ and $[PPN]^+$ with the iron carbonylate, may be in part responsible for this increased reactivity. Mössbauer effect data for the $[Et_4N]^+$ and $[PPN]^+$ salts are also reported.

Experimental section

Synthetic procedures

All manipulations were performed under an inert atmosphere of N_2 using standard Schlenk and vacuum line techniques. Solvents were dried by methods appropriate to each and deoxygenated. $[Et_4N]_2[Pb\{Fe(CO)_4\}_3]$ [7], $[Et_4N]_2[Fe_2(CO)_8]$ [1], $[PPN]_2[Fe_2(CO)_8]$ (PPN^+ = bis(triphenylphosphine)iminium) [1] were prepared by literature methods. The compound $[Et_4N]_2[Pb\{Fe(CO)_4\}_3]$ (1.0 g, 1.03 mmol) was reduced in tetrahydrofuran by adding a solution of sodium naphthalenide (0.106 g of Na, 0.60 g of naphthalene, 25 mL of tetrahydrofuran). A red solution resulted which was filtered affording a dark solid. Acetone and $[Et_4N]Br$ were added to the solid which was stirred for several hours. The resulting solution was filtered and cooled in the freezer yielding orange crystals of $[Et_4N]_2[Fe_2(CO)_8]$ contaminated with $[Et_4N]Br$. The latter was removed by washing the metal carbonyl with water and drying under vacuum. The yield of $[Et_4N]_2[Fe_2(CO)_8]$ was 71 mg (8%). ^{13}C NMR spectra were obtained on a Bruker 300 MHz NMR spectrometer in CD_3CN.

Mössbauer effect spectra

The Mössbauer effect spectra were obtained on a constant-accelerator spectrometer which utilized a room temperature rhodium matrix cobalt-57 source and was calibrated at room temperature with natural α-iron foil. The spectra of $[Et_4N]_2[Fe_2(CO)_8]$ were fit with a symmetric quadrupole doublet by using standard computer least-squares minimization techniques. In the case of $[PPN]_2[Fe_2(CO)_8]$ the components of the doublet were fit with equivalent linewidths but different areas. The different areas of the doublet result from texture in the absorber. Both absorbers contained 78 mg/cm^2 of the compound. The values of the isomer shift are accurate to *ca.* ± 0.005 mm/s and the values of the quadrupole splitting and linewidth are accurate to *ca.* ± 0.01 mm/s.

X-ray structure determination

Red-orange crystals of $[Et_4N]_2[Fe_2(CO)_8]$ formed upon cooling a concentrated acetone solution. A red prismatic crystal ($0.3 \times 0.2 \times 0.5$ mm^3) was mounted on a

glass fiber with epoxy cement. Crystal data were collected using Mo-K_α radiation ($(2\theta-\omega)$scans) on a Rigaku AFC5S four-circle diffractometer [8]. A full-matrix least-squares best fit of 25 random reflections between $6.99 \leq 2\theta \leq 14.29$ resulted in a primitive monoclinic unit cell with $a = 9.492(3)$, $b = 13.793(5)$, $c = 11.870(4)$ Å, $\beta = 112.81(2)°$, $V = 1432.5(8)$ Å^3. Three standard reflections were scanned every 150 reflections and showed an average decay of 2% at the end of data collection. Excluding standards, 1869 reflections were observed ($I > 3\sigma(I)$) for $+h$, $+k$, $\pm l$, ranging from h: 0 to 12, k: 0 to 18, l: −15 to 15 with $2\theta_{max} = 55°$ and $[(\sin\theta)/\lambda]_{max} = 0.65$. The structure was solved by using the program MITHRIL [9] which located the unique iron atom, followed by least-squares and Fourier analysis utilizing the TEXSAN (v. 2.0) structure analysis package [8] to find the remaining atoms. The hydrogens on the $[Et_4N]^+$ cation, which appeared in difference maps, were included in calculated positions during the final stages of refinement. Full-matrix least-squares refinement minimized $\Sigma w(|F_o| - |F_c|)^2$, where $w = [\sigma^2|F_o|]^{-1}$ (σ^2 = variance). The data were corrected for decay, absorption (DIFABS absorption correction [10]), and for Lp effects. All of the non-hydrogen atoms were refined anisotropically to $R = 0.032$, $R_w = 0.043$ with 163 variables, $(\Delta\rho)_{max} = 0.26$ e/Å^3, $(\Delta/\sigma)_{max} = 0.004$ and $S = 1.12$. Scattering factors were taken from standard sources [11].

Results and discussion

The reduction of main group–transition metal complexes which contain the main group atom in a central location and no transition metal–transition metal bonds leads most often to the cleavage of the main group–transition metal linkages [12]. The situation when transition metal–transition metal bonds are present is more complicated and often leads to novel rearrangements and unexpected, new cluster products. We were interested in adding electrons to $[Et_4N]_2[Pb\{Fe(CO)_4\}_3]$ as it is formally electron deficient and one can envisage a stable 4^- ion. Another possibility was the production of a dimetal system $[Pb\{Fe(CO)_4\}_2]^{2-}$ with loss of only one $[Fe(CO)_4]^{2-}$ group. Reduction of anionic complexes of this type has not been reported previously.

Use of sodium naphthalenide leads to cleavage of the main group–transition metal bonds as seen before for neutral complexes such as $Bi[Co(CO)_4]_3$. In our case, however, instead of forming the reduced *mononuclear* transition metal carbonylate, the dinuclear complex is produced. The reaction is very complicated and other tetrahydrofuran soluble metal carbonyl products are obtained which have not yet been identified.

The crystal structure of $[Et_4N]_2[Fe_2(CO)_8]$ has not been previously reported. The unit cell constants found in the initial crystallographic investigation were not recognized as being those of a known compound and the parameters would have easily fit the hypothetical $[Et_4N]_2[Pb\{Fe(CO)_4\}_2]$ complex mentioned above. The structure solution clearly showed that no lead was present and that the product was $[Et_4N]_2[Fe_2(CO)_8]$. The asymmetric unit $[Et_4N]_2[Fe_2(CO)_8]$ consists of two ordered cations per $[Fe_2(CO)_8]^{2-}$ anion. The $[Fe_2(CO)_8]^{2-}$ anion exhibits approximate D_{3d} symmetry as in the previous structures of the complex and is shown in Fig. 1. Selected positional parameters and bond distances and angles are given in Tables 1 and 2, respectively. The iron atoms are each coordinated to four

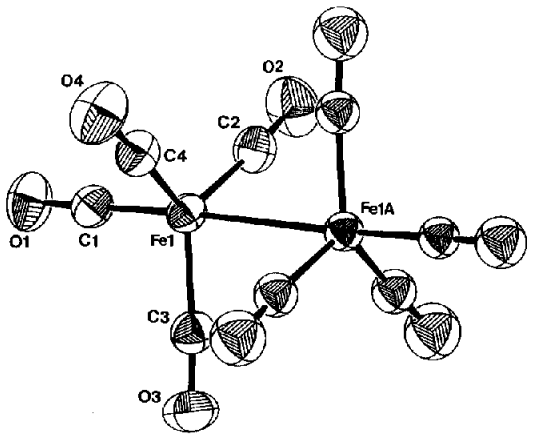

Fig. 1. ORTEP [20] diagram of $[Fe_2(CO)_8]^{2-}$.

carbonyls and are arranged in a trigonal bipyramidal fashion. A crystallographic inversion center sits at the midpoint of the Fe–Fe bond with the equatorial carbonyls tilted toward the center of symmetry. The Fe–Fe distance in $[Et_4N]_2[Fe_2(CO)_8]$ is 2.844(1) Å, significantly longer than the Fe–Fe distances in the $[PPN]^+ \cdot 2CH_3CN$ salt (2.787(2) Å) [2], the $[Fe(en)_3]^{2+}$ salt (2.75 Å) [4,13] and in the $[PPh_4]^+ \cdot 2CH_3CN$ salt (2.792(1) Å) [3]. If the electrostatic argument for the long bond distance in these compounds is correct, it suggests that the $[Et_4N]^+$ salt has even more charge built up at the metal center than in the other salts. The

Table 1

Selected positional parameters and B_{eq} for $[Et_4N]_2[Fe_2(CO)_8]$

Atom	x	y	z	B_{eq} [a]
Fe(1)	0.86507(5)	0.44253(3)	0.45972(4)	2.79(2)
O(1)	0.5875(3)	0.3285(2)	0.3886(2)	4.9(1)
O(2)	1.0422(3)	0.2863(2)	0.6185(3)	5.6(1)
O(3)	0.7412(3)	0.6022(2)	0.5559(2)	5.4(1)
O(4)	0.8567(3)	0.4465(2)	0.2105(2)	5.9(1)
C(1)	0.6980(3)	0.3745(2)	0.4163(3)	3.2(1)
C(2)	0.9787(3)	0.3513(2)	0.5582(3)	3.6(1)
C(3)	0.7971(3)	0.5406(2)	0.5199(3)	3.4(1)
C(4)	0.8664(3)	0.4479(2)	0.3109(3)	3.6(1)
N(1)	0.6463(3)	0.3742(2)	0.8048(2)	3.0(1)
C(1A)	0.8104(4)	0.3649(2)	0.8949(3)	3.7(1)
C(1B)	0.9266(4)	0.4142(3)	0.8577(3)	5.2(2)
C(1C)	0.6281(4)	0.3328(2)	0.6808(3)	4.1(1)
C(1D)	0.6702(5)	0.2279(3)	0.6814(3)	5.7(2)
C(1E)	0.5496(4)	0.3197(2)	0.8602(3)	4.2(1)
C(1F)	0.3795(4)	0.3204(3)	0.7843(5)	6.7(2)
C(1G)	0.5960(4)	0.4798(2)	0.7802(3)	3.9(1)
C(1H)	0.6004(5)	0.5353(3)	0.8899(4)	5.6(2)

[a] $B_{eq} = 8\pi^2/3(U_{11}aa^{*2}U_{22}bb^{*2} + U_{33}cc^{*2} + 2U_{12}aba^*b^* \cos\gamma + 2U_{13}aca^*c^* \cos\beta + 2U_{23}bcb^*c^* \cos\alpha)$.

Table 2

Selected intramolecular distances (Å) and angles (deg.) involving the non-hydrogen atoms of $[Et_4N]_2[Fe_2(CO)_8]$

Bond distances			
Fe(1)–C(1)	1.740(3)	N(1)–C(1A)	1.515(4)
Fe(1)–C(3)	1.765(3)	N(1)–C(1E)	1.520(4)
Fe(1)–C(2)	1.771(3)	N(1)–C(1C)	1.525(4)
Fe(1)–C(4)	1.773(3)	N(1)–C(1G)	1.525(4)
Fe(1)–Fe(1)*	2.844(1)	C(1A)–C(1B)	1.499(5)
O(1)–C(1)	1.159(3)	C(1C)–C(1D)	1.501(5)
O(2)–C(2)	1.160(4)	C(1E)–C(1F)	1.514(5)
O(3)–C(3)	1.167(4)	C(1G)–C(1H)	1.497(5)
O(4)–C(4)	1.159(4)		
Bond angles			
C(1)–Fe(1)–C(3)	95.7(1)	O(3)–C(3)–Fe(1)	174.8(3)
C(1)–Fe(1)–C(2)	93.7(1)	O(4)–C(4)–Fe(1)	174.4(3)
C(1)–Fe(1)–C(4)	94.9(1)	C(1A)–N(1)–C(1E)	106.3(2)
C(1)–Fe(1)–Fe(1)	177.2(1)	C(1A)–N(1)–C(1C)	110.6(2)
C(3)–Fe(1)–C(2)	120.2(1)	C(1A)–N(1)–C(1G)	112.1(2)
C(3)–Fe(1)–C(4)	121.1(1)	C(1E)–N(1)–C(1C)	111.8(3)
C(3)–Fe(1)–Fe(1)	81.9(1)	C(1E)–N(1)–C(1G)	111.0(2)
C(2)–Fe(1)–C(4)	116.7(1)	C(1C)–N(1)–C(1G)	105.3(2)
C(2)–Fe(1)–Fe(1)	86.3(1)	C(1B)–C(1A)–N(1)	115.2(3)
C(4)–Fe(1)–Fe(1)	87.6(1)	C(1D)–C(1C)–N(1)	115.2(3)
O(1)–C(1)–Fe(1)	179.1(3)	C(1F)–C(1E)–N(1)	115.0(3)
O(2)–C(2)–Fe(1)	174.0(3)	C(1H)–C(1G)–N(1)	114.9(3)

other metricals are nearly the same as those of the other reported salts except for the C(ax)–Fe–C(eq) angles which average 96.7(6)° in $[PPN]_2[Fe_2(CO)_8] \cdot 2CH_3CN$, 96.1(3.0)° in $[PPh_4]_2[Fe_2(CO)_8] \cdot 2CH_3CN$ but average 94.8(1.0)° in $[Et_4N]_2[Fe_2(CO)_8]$. For comparison, the metal–metal distance in the bridged carbonyl hydride, $[PPN][HFe_2(CO)_8]$, is 2.521(1) Å [14], and in $Fe_2(CO)_9$ the Fe–Fe bond length is 2.523(1) Å [15].

Because of the difference in the Fe–Fe bond lengths we sought to determine if other physical properties for the various salts might show some variation. Empirically the $[Et_4N]^+$ salt is much more air sensitive than the $[PPN]^+$ salt and this might be expected to lead to other differences in the solid state and perhaps even in solution. The ^{13}C NMR of the $[Et_4N]^+$ and $[PPN]^+$ salts were measured at room temperature in CD_3CN and found to be identical giving a single signal (δ 224.9 ppm) as expected for highly fluxional metal carbonyl complexes. Attempts at obtaining the Raman spectra of these two salts were not fruitful, probably due to the low Raman scattering power in general of metal carbonyl complexes. The Mössbauer effect spectra were obtained and did show some slight differences which are reported below.

The Mössbauer effect spectra of $[Et_4N]_2[Fe_2(CO)_8]$ and $[PPN]_2[Fe_2(CO)_8]$ measured at 78 K are shown in Fig. 2 and their hyperfine parameters are given in Table 3. The spectra obtained at 296 K are essentially identical to those shown in Fig. 2, except that the percent absorption is much reduced at 296 K. The very small absorption at the higher temperature required the use of rather thick samples, but there seems to have been little line broadening as a result. The hyperfine

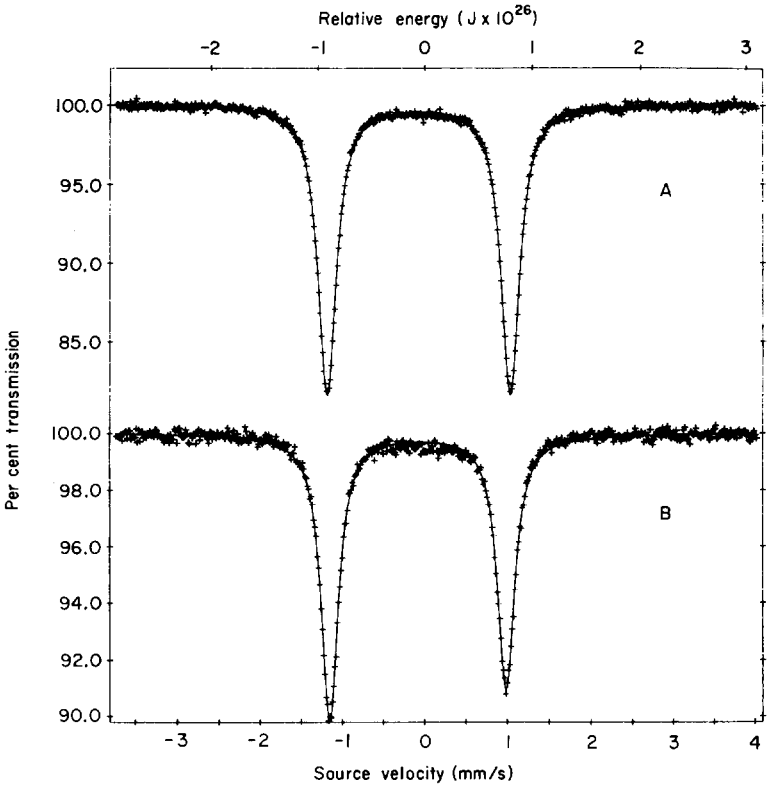

Fig. 2. Mössbauer effect spectra of $[Et_4N]_2[Fe_2(CO)_8]$ (A) and $[PPN]_2[Fe_2(CO)_8]$ (B), obtained at 78 K.

parameters for $[Et_4N]_2[Fe_2(CO)_8]$ have been reported earlier [16] and the results reported in Table 3 are virtually identical to those reported earlier. This compound has been remeasured to obtain the hyperfine parameters with a higher accuracy for direct comparison with $[PPN]_2[Fe_2(CO)_8]$. Such a direct comparison was necessary to see if there were any distinct differences in the spectra for the two compounds that might result from the different Fe–Fe bond distances.

The structures of the anions in the $[Et_4N]^+$ and $[PPN]^+$ salts are very similar as a comparison of Table 2 with Table 1 in reference 2 reveals. As mentioned above, the main difference is the Fe–Fe bond which is 0.06 Å or 2% longer in the

Table 3

Mössbauer effect spectral parameters

Compound	T (K)	δ_1 [a] (mm/s)	ΔE_Q (mm/s)	Γ (mm/s)	Area (%ϵ) (mm/s)
$[Et_4N]_2[Fe_2(CO)_8]$	296	−0.156	2.18	0.24	3.80
	78	−0.073	2.22	0.27	15.13
$[PPN]_2[Fe_2(CO)_8]$	296	−0.165	2.10	0.23	1.11
	78	−0.081	2.14	0.25	7.42

[a] The isomer shift is measured relative to room temperature α-iron foil.

$[Et_4N]^+$ salt. In contrast the iron to carbonyl–carbon bond distances are virtually identical and the bonding angles at the iron are very similar. Apparently the longer Fe–Fe distance in the $[Et_4N]^+$ salt results in a small decrease in the electronic symmetry at the iron, which in turn increases slightly the quadrupole splitting at the iron when compared with the $[PPN]^+$ salt. The similarity of the iron–ligand bond distances also accounts for the very similar isomer shifts found in the two compounds. Apparently the increase in the Fe–Fe bond distance in $[Et_4N]_2[Fe_2(CO)_8]$ reduces the Fe–Fe bonding interaction slightly, reduces the 4*s* electron density overlap slightly and, consequently, increases the isomer shift slightly. However, it should be noted that the difference in the isomer shifts, while probably real, is of the order of the accuracy in the numbers.

From the temperature dependence of the isomer shift and the logarithm of the absolute absorption area, it is possible to obtain values for the effective Mössbauer absorber mass [17,18]. For $[Et_4N]_2[Fe_2(CO)_8]$ and $[PPN]_2[Fe_2(CO)_8]$, the respective values are 109 and 109 g/mol for the absorber mass, 105 and 91 K for the effective temperature. These results, which should be considered as approximate because they are based on only two data points, are very typical for this type of compound [17,19] and reveal the expected similarities for the bonding in the two compounds.

Acknowledgments

K.H.W. thanks the National Science Foundation for support of this work and for support in the purchase of the Rigaku AFC5S automated diffractometer. G.J.L. thanks the donors of the Petroleum Research Fund, administered by the American Chemical Society for their support of this research. Dr. Carolyn M. Jones is acknowledged for the acquisition of the ^{13}C NMR spectra and Professor D.F. Shriver for attempting the Raman analysis.

References

1 C.E. Sumner, Jr., J.A. Collier and R. Pettit, Organometallics, 1 (1982) 1350.
2 H.B. Chin, M.B. Smith, R.D. Wilson and R. Bau, J. Am. Chem. Soc., 96 (1974) 5285.
3 N.K. Bhattacharyya, T.J. Coffy, W. Quintana, T.A. Salupo, J.C. Bricker, T.B. Shay, M. Payne and S.G. Shore, Organometallics, 9 (1990) 2368.
4 F.S. Stephens, Acta Crystallogr., Sect. A, 21 (1966) 154.
5 M. Darensbourg and C. Borman, Inorg. Chem., 15 (1976) 3121.
6 M.Y. Darensbourg, D.J. Darensbourg, D. Burns and D.A. Drew, J. Am. Chem. Soc., 98 (1976) 3127.
7 J.M. Cassidy and K.H. Whitmire, Inorg. Chem., 28 (1989) 2494.
8 (a) Molecular Structure Corporation, 1988a. CONTROL(4:0:0). Program for data collection, Mol. Str. Corporation MSC, 3200A Research Forest Drive, The Woodlands, TX 77381, USA, 1988; (b) TEXRAY Structure Analysis Package, Version 2.1., MSC, 3200A Research Forest Drive, The Woodlands, TX 77381, USA, 1988.
9 C.J. Gilmore, MITHRIL. A Computer Program for the Automatic Solution of Crystal Structures from X-ray Data, University of Glasgow, Scotland, 1983.
10 N. Walker and D. Stuart, Acta Crystallogr., Sect. A 39 (1983) 158.
11 D.T. Cromer and J.T. Waber, International Tables for X-ray Crystallography, Vol. IV, Kynoch Press, Birmingham, 1974, p. 71 (scattering factors), p. 148 (anomalous dispersion) (present distributor Kluwer Academic Publishers, Dordrecht).
12 K.H. Whitmire, J. Coord. Chem. B, 17 (1988) 95.
13 L.B. Handy, J.K. Ruff and L.F. Dahl, J. Am. Chem. Soc., 92 (1970) 7312.
14 H.B. Chin and R. Bau, Inorg. Chem., 17 (1978) 2314.

15 F.A. Cotton and J.M. Troup, J. Chem. Soc., Dalton Trans., (1974) 800.
16 K. Farmery, M. Kilner, R. Greatrex and N.N. Greenwood, J. Chem. Soc. A, (1969) 2339.
17 R.H. Herber, in R.H. Herber (Ed.), Chemical Mössbauer Spectroscopy, Plenum, New York, 1984, pp. 199–216.
18 R.D. Ernst, D.R. Wilson and R.H. Herber, J. Am. Chem. Soc., 106 (1984) 1646.
19 G.J. Long, unpublished results.
20 C.K. Johnson, ORTEP-II. Report ORNL-5138, Oak Ridge National Laboratory, Tennessee, USA, 1976.